Damage characteristics of HfO_2/SiO_2 high reflector at 45° incidence in 1-on-1 and N-on-1 tests

Xiaofeng Liu (刘晓凤)[1,2*], Dawei Li (李大伟)[1], Yuan'an Zhao (赵元安)[1], Xiao Li (李 笑)[1,2], Xiulan Ling (凌秀兰)[1,2], and Jianda Shao (邵建达)[1]

[1]*Shanghai Institute of Optics and Fine Mechanics, Chinese Academy of Sciences, Shanghai 201800, China*

[2]*Graduate School of the Chinese Academy of Sciences, Beijing 100049, China*

[*]*E-mail: xiaofeng198225@163.com*

Received February 26, 2009

P-polarization high reflectors are deposited by e-beam from hafnia and silica. 1-on-1 and N-on-1 tests at 1064-nm wavelength with P-polarization at 45° incidence are carried out on these samples. Microscope and scanning electron microscope are applied to investigate the damage morphologies in both 1-on-1 and N-on-1 tests. It is found that the laser damage threshold is higher in N-on-1 tests and nodular defect is the main inducement that leads to the damage because nodular ejection with plasma scalding is the typical damage morphology. Similar damage morphology observed in the two tests indicates that the higher laser damage threshold in N-on-1 test is attributed to the mechanical stabilization process of nodular defects, owing to the gradually increased laser fluence radiation. Based on the typical morphology study, some process optimizations are given.

OCIS codes: 140.3330, 310.0310.

doi: 10.3788/COL20100801.0041.

The output of high peak-power laser is often limited by the damage threshold of multilayer dielectric coatings used in the system. Sub-threshold illumination attracts people's attention as it can make some coatings reach the damage standard, which is hard to be achieved by the current coating technologies. However the mechanisms that lead to the damage in laser illumination process and the improvement of laser damage threshold in sub-threshold illumination process are not well understood. Damage morphologies are one of the most intuitional and principal evidences for the relevant mechanisms studies[1−5]. In previous laser damage threshold test experiments, the enhanced thresholds are always discussed[6−14], while damage morphologies in these threshold enhancement processes are not presented in detail[9].

In order to investigate the damage properties of the typical defects and the reason for the enhancement of laser damage resistance in the N-on-1 test, in this letter, we will focus on the typical damage morphologies found in HfO_2/SiO_2 multilayer mirrors after 1-on-1 and N-on-1 tests. Understanding such information is helpful not only to study laser damage and laser conditioning mechanisms, but also to improve the laser damage threshold effectively and efficiently.

All mirrors were prepared by e-beam deposition of hafnia and silica with a high purity of 99.9999% onto BK7 substrates in a ZZSX-800F coating equipement. Both of the two coating materials are produced by General Research Institute of Nonferrous Metals. The coating designs of these samples are $(2H2L)^{16}$ 2H4L. They are designed to operate at the incidence of 45° and reflect highly at the wavelength of 1064 nm for P-polarization. The actually measured spectrum is shown in Fig. 1.

Laser damage threshold tests are carried out using a 9-ns pulse from a 1064-nm ND: YAG Laser. The tests are conducted under P-polarization illumination at 45° incidence. The effective area of the spot that irradiated on the sample is 0.572 mm^2 at normal incidence, which means it is 0.8 mm^2 at 45° incidence. For each shot, energy and spot are recorded. So as not to effect neighbor test sites, the distance between two adjacent test sites is 3 mm both in X and Y direction. The measurement, either 1-on-1 or N-on-1, is done on each sample. Any visible change that could be seen under Nomarski microscope of 100× magnification is considered as damage. In the N-on-1 test, once the damage has occurred, stop irradiating this site and start irradiating the next site with the same process.

The results of laser damage threshold tests are shown in Fig. 2. According to ISO11254-1, in which laser damage threshold is determined by a linear extrapolation of the damage probability data to zero damage probability, the laser damage threshold of 1-on-1 is 7.6 J/cm^2. However, there is no standard definition for N-on-1 laser damage threshold. In order to ensure the accuary of measurement, four samples that irradiated by the

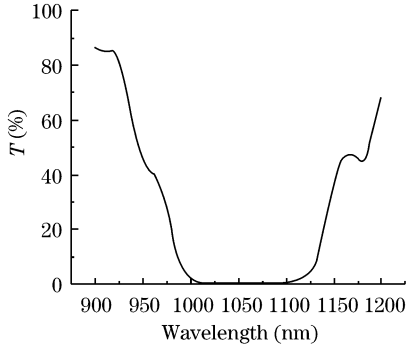

Fig. 1. Transmission spectrum measured by a Lambda900 spectrophotometer.

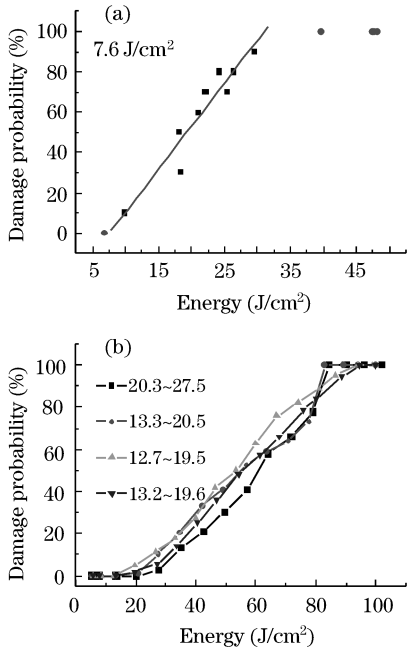

Fig. 2. Results of laser damage threshold test of (a) 1-on-1 test and (b) N-on-1 test. The start energy is about 5 J/cm^2.

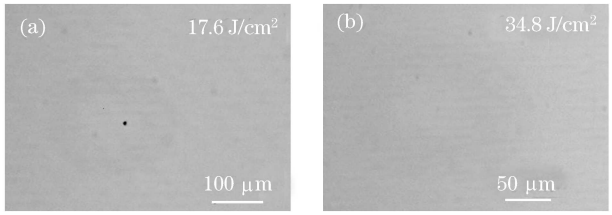

Fig. 3. Typical damage morphologies taken by a Nomarski microscope. Damage appeared in (a) 1-on-1 test and (b) N-on-1 test.

approximate energy steps are tested. In Fig. 2(b), it is obviouse that the damage threshold of zero damage probability is above 12.7 J/cm^2 for the presence of laser conditioning effect.

Observed under the Nomarski microscope, damage morphologies in each test are similar to some extent. Damage appears as surface discoloration with or without a pit in it as shown in Fig. 3, and the surface discoloration with a pit plays a dominate role absolutely. No further information can be obtained from the microsopic pictures. But more details are revealed by the pits when scanning electron microscope (SEM) is applied.

Surface discoloration under the microscope can be seen more clearly under SEM. It looks brighter because of its rougher surface. In our study, most pits are similar to those in Fig. 4(b) and are all formed by nodular ejection in substance[5]. Only few pits, called as flat-bottom pits, are observed as the ones shown in Fig. 4(d), and a smaller absorbing center with a diameter of nanometer scale always locates in the center of such pit. Surface discoloration without a pit is shown in Fig. 4(e).

In 1-on-1 test, most of the pits inside surface discolorations observed by SEM are caused by nodular ejection, as shown in Fig. 5(b). Surface discoloration without a pit shown in Fig. 5(c) also exists but no flat-bottom pit

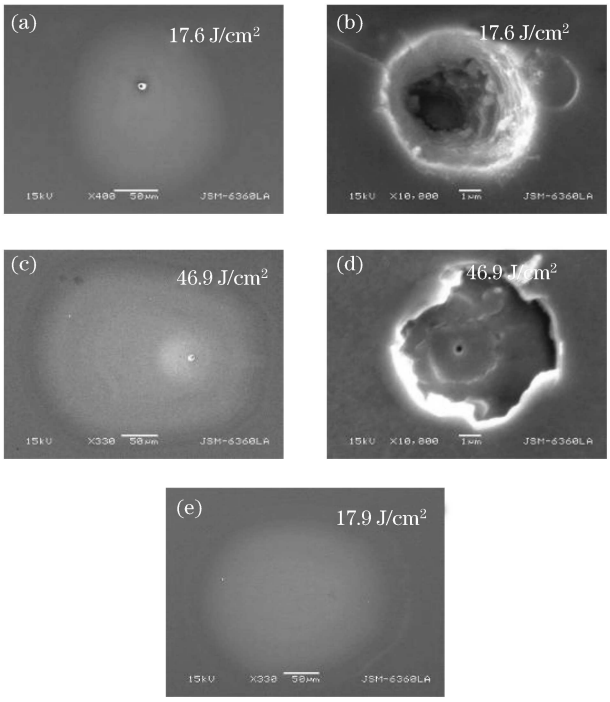

Fig. 4. Three kinds of typical damage morphologies appeared in 1-on-1 test. (a), (c), and (e) are the SEM images of the whole damage region; (b) and (d) are the SEM images of the pits in (a) and (c), respectively.

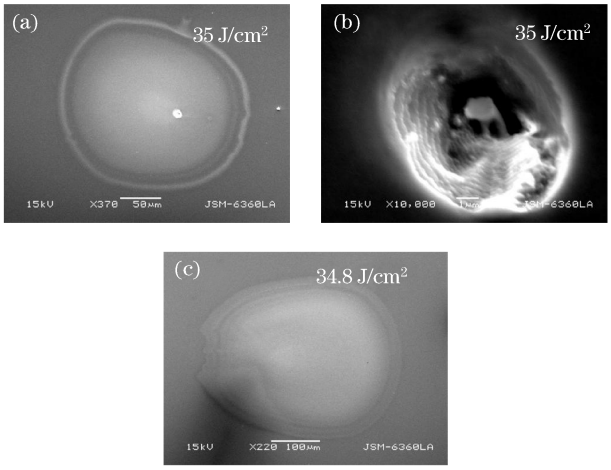

Fig. 5. Different damage morphologies under approximate energy steps in N-on-1 tests; (b) is the SEM image of the pit in (a).

is observed.

No matter in 1-on-1 or N-on-1 test, we found some irregular-shaped damage pits that retained most characteristics of nodular ejection but not to be exactly cone-shaped, as shown in Fig. 6, and the pit images taken by SEM indicate that more than one circular seeds located closely in these regions or noncircular seeds existed.

From our damage experiments, it is safe to conclude that the typical damage in these coatings is induced by nodular defect. The typical damage morphology is the result of laser interaction with the mechanically unstable coating defect. For some damage sites shown in Fig. 7, owing to the incidence angle of 45°,

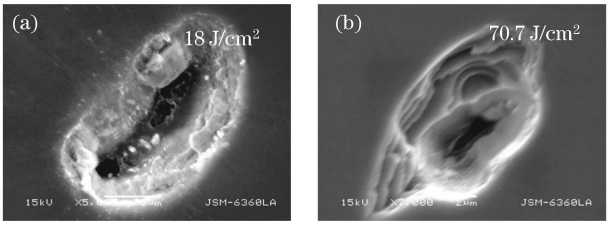

Fig. 6. Irregular-shaped damage pits damage morphology in (a) 1-on-1 test and (b) N-on-1 test.

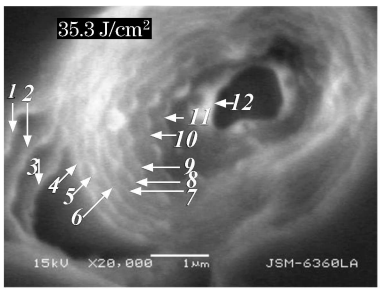

Fig. 7. Damage layer number of a pit.

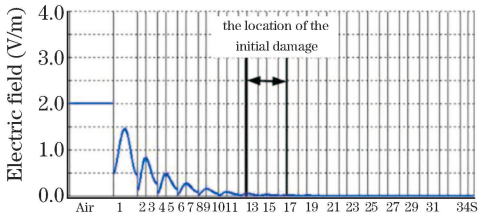

Fig. 8. Electric field distribution versus film layer number.

Table 1. Statistical Results of the Initial Damage Layers.

Energy (J/cm^2)	17.9	24	35.3	71.2
Layer of the Deepest Damage (N)	15	16	12	14

we can count out the layers from the edge of pits easily at a higher magnification. Each sample is comprised of 34 layers, and we treat the first layer as the one exposed to the air. Table 1 lists the initial damage layer of four damage sites, that is to say, the location of the seed. It is found that the initial damage locations are close. Such information can be very important to the operator of the coating apparatus, because it might be correlated to a particular deposition event. If special treatment was given to the deposition of these layers, such defects could be reduced, and therefore laser damage resistance could be enhanced. In theory, the electric field is very low at the location of the initial damage layer, nearly zero, as shown in Fig. 8. Such deep seed ejection suggests that the present of nodular defect acts as micro-lens[15] in the coating and the electric field intensity in the vicinity of the nodular seed is enhanced significantly[16], which creates localized heat enhancement .These localized hot spots will cause affected regions to expand rapidly resulting in areas of high compressive stress surrounded by thin layers of tensile stress. The highest tensile stresses are located around the seed and at the surface of the nodule along the centerline[17] Besides that, the boundaries of these nodules may have stresses associated with them, which can be relieved by nodular ejection. The shadowing effect responsible for the nodule growth may also result in the formation of a void between the nodule and the surrounding film, allowing the nodule to become loose in the film[18]. So fracture of the nodule would be initiated at either of these two locations. Surface discolorations are attributed to plasma scalds. The reason for plasma scalding without a pit is that a defect-free region is illuminated and damage is induced by surface high electric field. Plasmas can be created by phase transformation in the process of nodular ejection and high electric field on the coating surface or contamination.

Flat-bottom pit is not common in our study. Perhaps because of limited sample sits, or being transformed to plasma scalds without pits as the previous experiments have proved[3], flat-bottom pit damage is observed in N-on-1 tests.

Typical damage in N-on-1 tests, which is similar to the one in 1-on-1 tests, does not occur until a higher energy illuminates. This phenomenon suggests that the mechanical stabilization process of defects should be responsible for the improved laser damage threshold in N-on-1 tests. The slowly increased energy may fuse the nodular defect into the coating, therefore increases its mechanical stability. Nodular seed needs more thermal stress to break the bound of the adjacent films. The stabilization process does not conflict with the most popular theory that the relationship between nodular defect and laser conditioning is defect removing mechanism[19]. The absence of potentially absorbing nodular seeds and absorption reductions up to 150 × have been observed[20]. However, mechanical stabilization effect is limited for nodular seeds, and film components are used many times in work enviroment. Once optics that only through such mechanical stabilization treatment were conducted in real work condition, nodular seeds still could absorb much heat and cause catastrophic damage. So removing the damage source becomes the final goal for laser condition. The sizes of such pits in the two tests are all several microns, that is to say, this stability process in N-on-1 does not change the damage , caused by nodular seeds, in size. If more other test results about the above damage regions in these two tests change little, we can cancel the stabilization process of nodular defects under lower energy irradiation, and implement the one step illumination by choosing proper energy step to remove the seed directly.

In conclusion, laser damage threshold is higher in N-on-1 test, which can be attributed to the mechanical stabilization of defects. Similar damage morphologies are found in different tests. Nodular defects are dominant in these samples and are very susceptive to the laser. Process optimization about deposition and laser conditioning is offered.

This work was supported by the National “863” Program of China under Grant No. 2006AA804908.

References

1. D. Li, Y. Zhao, J. Shao, Z. Fan, and H. He, Chin. Opt. Lett. **6,** 386 (2008).

2. C. Xu, H. Dong, J. Ma, Y. Jin, J. Shao, and Z. Fan, Chin. Opt. Lett. **6,** 228 (2008).
3. X. Liu, D. Li, X. Li, Y. Zhao, and J. Shao, Chinese J. Lasers (in Chinese) **36,** 1 (2009).
4. S. C. Weakley, C. J. Stolz, Z. Wu, R. P. Bevis, and M. K. von Gunten, Proc. SPIE **3578,** 137 (1999).
5. F. Y. Génin and C. J. Stolz, Proc. SPIE **2870,** 439 (1996).
6. C. R. Wolfe, M. R. Kozlowski, J. H. Campbell, F. Rainer, A. J. Morgan, and R. P. Gonzales, Proc. SPIE **1438,** 360 (1989).
7. M. R. Kozlowski, C. R. Wolfe, M. C. Staggs, and J. H. Campbell, Proc. SPIE **1438,** 376 (1989).
8. M. R. Kozlowski, M. Staggs, F. Rainer, and J. H. Stathis, Proc. SPIE **1441,** 269 (1991).
9. M. C. Staggs, M. Baloch, M. R. Kozlowski, and W. J. Siekhaus, Proc. SPIE **1624,** 375 (1992).
10. Z. L. WU, Z. X. Fan, and D. Schäter, Proc. SPIE **1624,** 362 (1992).
11. L. Sheehan, M. Kozlowski, F. Rainer, and M. Staggs, Proc. SPIE **2114,** 559 (1994).
12. Q. Zhao, H. Qiu, Y. Liu, Z. Fan, and Z. Wang, Acta Opt. Sin. (in Chinese) **19,** 1105 (1999).
13. Y. Zhao, T. Wang, D. Zhang, S. Fan, J. Shao, and S. Fan, Appl. Surf. Sci. **239,** 171 (2005).
14. J. Capoulade, L. Gallais, J.-Y. Natoli, and M. Commandré, Appl. Opt. **47,** 5272 (2008).
15. J. Murphy, Proc. SPIE **246,** 64 (1980).
16. C. J. Stolz, F. Y. Génin, and T. V. Pistor, Proc. SPIE **5273,** 41 (2004).
17. R. H. Sawicki, C. C. Shang, and T. L. Swatloski, Proc. SPIE **2428,** 333 (1995).
18. M. R. Kozlowski, M. Staggs, M. Balooch, R. Tench, and W. Siekhaus, Proc. SPIE **1556,** 68 (1991).
19. A. Fornier, C. Cordillot, D. Ausserre, and F. Paris, Proc. SPIE **2253,** 817 (1994).
20. A. B. Papandrew, C. J. Stolz, Z. L. Wu, G. E. Loomisa, and S. Falabella, Proc. SPIE **4347,** 53 (2001).